Design of an Improved MPPT Control of DFIG Wind Turbine under Unbalanced Grid Voltage using a Flux Sliding Mode Observer

Youssef Majdoub[1], Ahmed Abbou[2], Mohamed Akherraz[3], Rachid El Akhrif[4]
Mohammed V University Agdal, Mohammadia School of Engineers, Agdal Rabat, Morocco

Article Info	ABSTRACT
	This study presents a control scheme of the electronic interface of a grid connected Variable Speed Wind Energy Generation System (VS-WEGS) based on a Doubly Fed Induction Generator (DFIG). The efficiency of the wind energy is represented to according to the control strategy applied. Thus, in the case of unbalanced grid voltage, the negative sequence voltage causes additional strong oscillation at twice the grid frequency in the stator instantaneous active and reactive powers. The objective of this work is to present an enhanced MPPT controller uses backstepping approach implemented in both dq^+ and dq^- reference frames rotating to keep a safe operation of DFIG during unbalanced grid voltage associated with regulating rotor flux, in order to estimate rotor flux, a nonlinear observer based on sliding mode is proposed in this work. Note that the conventional controllers (PI, PI-R …) are not provided satisfactory performance during unbalanced voltage dips. The validation of results has been performed through simulation studies on a 4 kW DFIG using Matlab/Simulink

Corresponding Author:

Youssef Majdoub,
Mohammadia School of Engineers,
Mohammed V University Agdal,
Agdal Rabat, Morocco
Email: youssef_maj@hotmail.com

1. INTRODUCTION

Wind power system can be exploited at constant speed or variable speed operations using power electronic converters. In this work, the wind turbine will be exploited at the maximum power operating point (MPPT) for various wind speeds by optimally controlling the speed of the shaft [1]. In contrast, regulating the rotor flux need the state vector of the controlled system.Thus, a good knowledge of the rotor flux is a necessity [2]-[3]-[4].Hence; the use of a physical sensor introduces a lot of problem in maintenance, quality of service, precision and cost. To overcome this difficulty, preceding works present the observer for flux estimation, then the speed is estimated from flux [5] – [6].Indeed; different models have been proposed for estimating rotor flux. One distinguishes for example statistical models (e.g. [7]). The proposed estimators generally show a complex processing mode and, therefore, lead to serious implementation problems in real time. For this purpose, the Sliding Mode Observer presented in this article will be based on measuring machine currents and voltages only.

However, the unbalanced network voltages have detrimental effects on the operation of the DFIG when the stator is directly connected to the grid as in our case study [8]. In this sense, and due to the strong penetration of DFIG into wind turbine structures, much research in recent years has sought to improve robust and accurate control under various network disturbances [9]-[10]-[11]. With the increasing use of wind power, it has become unacceptable to accept disconnection of the wind turbine with each occurrence of a fault on the electrical grid. This disconnection could result in a large number of undistributed energy, which

favors network instability. However, the grid voltage has been assumed symmetrical for many works. While in practice, asymmetric faults are often present. For a DFIG generator, if the unbalanced voltage has not been taken into account in the control law, with a shallow depth, high pulses can be obtained at twice the grid frequency appearing in the torque electromagnetic, active and reactive powers of the stator, which implies the separation of the wind turbine system of the grid [9]-[12]-[13]. In [14]-[15] the PI controllers are used to control the DFIG under unbalanced condition. Some authors use PI-R controller where the positive synchronous reference frame can directly regulate both positive and negative sequence components without involving sequential decomposition [16]. Moreover, some strategies such as DPC based on power definition connected to unbalanced grid voltage are proposed with reduced double grid frequency oscillations of electromagnetic torque [17]-[18], but despite the simplicity of these controllers, they are not enough at the point of precision.

In this work, the performance of the wind integration under unbalanced grid has been enhanced by the elimination of oscillations indueced by the asymmetric voltage, based on rotor flux sliding mode observer. The paper is organized as follows: the wind turbine modeling under unbalanced grid voltage is presented in section 2. Section 3 is devoted to design of the rotor flux sliding mode observer and controllers' laws. The control performance is shown by simulation in Section 4, a conclusion and reference list end the paper

2. WIND TURBINE MODEL UNDER UNBALANCED GRID
2.1. Turbine model
The turbine model is inspired from [1]. The available aerodynamic wind power is given by:

$$P_{aero} = \frac{1}{2}\rho\pi R^2 C_P(\lambda, \beta)v_w^3 \tag{1}$$

Where β is a blade pitch angle, in this paper, β is held constant ($C_P(\lambda, \beta) \stackrel{def}{=} C_P(\lambda)$), $C_P(\lambda)$ is the coefficient of performance, v_w is the wind velocity, ρ is the air density, R is the radius of the wind turbine rotor and the tip speed ratio λ is given by

$$\lambda = \frac{R\omega_t}{v_w} \tag{2}$$

2.2. Dynamic DFIG model with iron losses
The equivalent circuit of a DFIG is inspired from the proposed model in [19]-[20] .When the iron loss resistance R_m is connected in parallel with the stator inductance ($L_{s\sigma}$ and M). The choice of this model is justified mainly by the simplicity of calculations, because we will have a similar circuit to the conventional model (without iron losses) using thevenin's theorem. The equivalent circuit of the DFIG after arrangement is shown in Figure 1. In addition, the R_m resistance is a variable parameter.The Thevenin's equivalents for stator resistance and voltages/currents are calculated in the stationary, α- β reference frame as follows [19]-[20]-[21].

$$R_{sT} = \frac{R_s R_m}{R_s + R_m} \; ; \; v_{sT\alpha} = \frac{R_m}{R_s + R_m}v_{s\alpha} \; ; \; v_{sT\beta} = \frac{R_m}{R_s + R_m}v_{s\beta} \; ; \; i_{sT\alpha} = \frac{R_s + R_m}{R_m}i_{s\alpha} + \frac{v_{s\alpha}}{R_m} \; ; \; i_{sT\beta} = \frac{R_s + R_m}{R_m}i_{s\beta} + \frac{v_{s\beta}}{R_m} \tag{3}$$
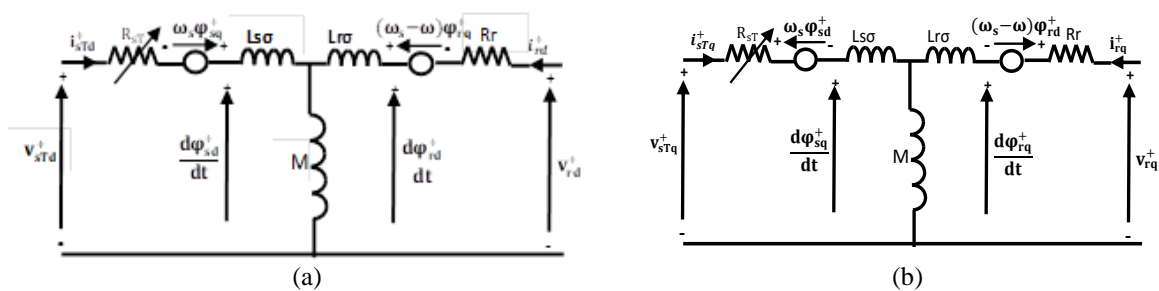

(a) (b)

Figure 1. DFIG equivalent circuit in the dq^+ reference frame: (a) direct axis, (b) quadrature axis [19]

The model considered for DFIG can be written as follows:

$$\begin{cases} \dot{x} = f(x,u,w) \overset{\text{def}}{=} [f_1(x,u,w) \ f_2(x,u,w) \ ... \ f_5(x,u,w)]^T \\ y = h(x) \overset{\text{def}}{=} [h_1(x) \ h_2(x) \ h_3(x)]^T \end{cases} \text{with} \begin{cases} x = [i^+_{sTd} \ i^+_{sTq} \ \varphi^+_{rd} \ \varphi^+_{rq} \ \Omega]^T \\ u = [\ v^+_{sTd} \ v^+_{sTq}\ ]^T \text{ and } \ w = \end{cases}$$
$$[\ v^+_{rd} \ v^+_{rq}\ ]^T$$

$$\begin{cases} f_1(x,u,w) = -\eta i^+_{sTd} + \omega_s i^+_{sTq} + \alpha\beta\varphi^+_{rd} + \beta\omega\varphi^+_{rq} + \frac{1}{\sigma L_s}V^+_{sTd} - \beta V^+_{rd} \\ f_2(x,u,w) = -\omega_s i^+_{sTd} - \eta i^+_{sTq} - \beta\omega\varphi^+_{rd} + \alpha\beta\varphi^+_{rq} + \frac{1}{\sigma L_s}V^+_{sTq} - \beta V^+_{rq} \\ f_3(x,u,w) = \alpha M i^+_{sTd} - \alpha\varphi^+_{rd} + g\omega_s\varphi^+_{rq} + V^+_{rd} \\ f_4(x,u,w) = \alpha M i^+_{sTq} - g\omega_s\varphi^+_{rd} - \alpha\varphi^+_{rq} + V^+_{rq} \\ f_5(x,u,w) = \frac{\mu}{J}\left(\varphi^+_{sq}i^+_{rd} - \varphi^+_{sd}i^+_{rq}\right) - \frac{f}{J}\Omega + \frac{T_m}{J} \end{cases} \qquad (4)$$

Where: $\sigma = 1 - \frac{M^2}{L_r L_s}; \eta = \left(\frac{1}{\sigma T_s} + \frac{1-\sigma}{\sigma T_r}\right); \ \alpha = \frac{R_r}{L_r}; \ \beta = \frac{1-\sigma}{\sigma M}; \ T_s = \frac{L_s}{R_s}; T_r = \frac{L_r}{R_r}; \ \mu = \frac{PM}{L_s}$

Ω : DFIG rotor speed; J : total inertia constant;   f : viscous friction coefficient; (L_s, L_r, M): Stator, rotor and mutual cyclic inductance; $(L_{s\sigma}, L_{r\sigma})$: stator ,rotor cyclic leakage inductance ; (R_s, R_r): stator and rotor resistances ; (φ_s, φ_r): stator , rotor flux components ; Superscripts (+, -): positive, negative reference frame ; Subscripts (+, -) : positive, negative sequence component .

Figure 2 presents the spatial relationships between the stationary (αβ)s reference frame, the rotor (αβ)r rotating at the speed of ω_r, and the dq$^+$ and dq$^-$ reference frames rotating at the angular speed of ω_s and $-\omega_s$, respectively.

$$f^+_{dq} = f_{(\alpha\beta)_s}e^{-j\omega_s t} \ ; \ f^-_{dq} = f_{(\alpha\beta)_s}e^{j\omega_s t}; f^+_{dq} = f_{(\alpha\beta)_r}e^{-j\omega_{slip+}t} \ ; \quad f^-_{dq} = f_{(\alpha\beta)_r}e^{-j\omega_{slip-}t}$$

Where: f represents the voltage (current and flux), $\omega_{slip+} = \omega_s - \omega$ and $\omega_{slip-} = -\omega_s - \omega$

According to (4), the stator current can be calculated as:

$$i^+_{sTdq} = \frac{\varphi^+_{sdq} - Mi^+_{rdq}}{L_s} \qquad (5)$$

From (4) and (5), the rotor flux can be written

$$\varphi^+_{rdq} = \frac{M\varphi^+_{sdq}}{L_s} + L_r\sigma i^+_{rdq} \qquad (6)$$

Substituting (6) into (4) yields the rotor voltage in the dq$^+$ reference frame as

$$v^+_{rdq} = R_r i^+_{rdq} + \frac{M}{L_s}\frac{d\varphi^+_{sdq}}{dt} + L_r\sigma\frac{di^+_{rdq}}{dt} + j\omega_{slip+}\left(\frac{M\varphi^+_{sdq}}{L_s} + L_r\sigma i^+_{rdq}\right) \qquad (7)$$

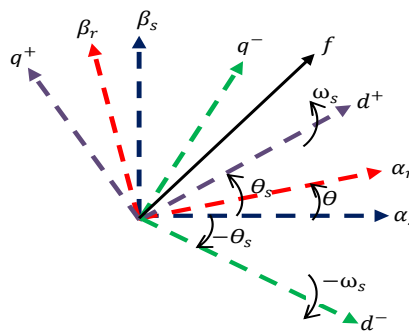Figure 2. Relationships between stationary (αβ)s reference frame, the rotor (αβ)r reference frame

2.3. Instantaneous active and reactive power flow under unbalanced grid

By neglecting the stator resistance voltage drop and considering (4), the stator voltage can be represented in the positive dq^+ reference frame as [19]

$$v_{sTdq}^+ \approx j\omega_s(\varphi_{sdq+}^+ - \varphi_{sdq-}^- e^{-j2\omega_s t}) \tag{8}$$

According to (8), the stator flux in the positive dq^+ reference frame can be expressed evidently as:

$$\varphi_{sdq}^+ = \frac{-j}{\omega_s}(v_{sTdq+}^+ - v_{sTdq-}^- e^{-j2\omega_s t} \tag{9}$$

Under unbalanced grid voltage conditions, the instantaneous active and reactive power outputs from DFIG stator can be expressed in (10) with $\bar{i}_{sTdq}^+$ is the conjugate complex of i_{sTdq}^+ :

$$P_s + jQ_s = v_{sTdq}^+ \times \bar{i}_{sTdq}^+ \tag{10}$$

Substituting (5), (8) and (9) into (10) and separating the instantaneous active and reactive powers into different pulsating components yield [19]:

$$P_s = P_{s0} + P_{s-\sin2}\sin(2\omega_s t) + P_{s-\cos2}\cos(2\omega_s t) \tag{11.a}$$

$$Q_s = Q_{s0} + Q_{s-\sin2}\sin(2\omega_s t) + Q_{s-\cos2}\cos(2\omega_s t) \tag{11.b}$$

Where,

$$
\text{Where,}\quad
\begin{bmatrix} P_{s0} \\ Q_{s0} \\ P_{s\sin2} \\ P_{s\cos2} \\ Q_{s\sin2} \\ Q_{s\cos2} \end{bmatrix}
= -\frac{\omega_s}{L_s}
\begin{bmatrix}
0 & 0 & 0 & 0 \\
-\varphi_{sd}^+ & -\varphi_{sq}^+ & \varphi_{sd-}^- & \varphi_{sq-}^- \\
\varphi_{sd-}^- & \varphi_{sq-}^- & \varphi_{sd+}^+ & \varphi_{sq+}^+ \\
-\varphi_{sq-}^- & \varphi_{sd-}^- & \varphi_{sq+}^+ & -\varphi_{sd+}^+ \\
0 & 0 & 0 & 0 \\
0 & 0 & 0 & 0
\end{bmatrix}
\begin{bmatrix} \varphi_{sd+}^+ \\ \varphi_{sq+}^+ \\ \varphi_{sd-}^- \\ \varphi_{sq}^- \end{bmatrix}
- \frac{M}{L_s}
\begin{bmatrix}
v_{sTd+}^+ & v_{sTq+}^+ & v_{sTd-}^- & v_{sTq-}^- \\
v_{sTq+}^+ & -v_{sTd+}^+ & v_{sTq-}^- & -v_{sTd-}^- \\
v_{sTq-}^- & -v_{sTd-}^- & -v_{sTq+}^+ & v_{sTd+}^+ \\
v_{sTd-}^- & v_{sTq-}^- & v_{sTd+}^+ & v_{sTq+}^+ \\
-v_{sTd-}^- & -v_{sTq-}^- & v_{sTd+}^+ & v_{sTq+}^+ \\
v_{sTq-}^- & -v_{sTd-}^- & v_{sTq+}^+ & -v_{sTd+}^+
\end{bmatrix}
\begin{bmatrix} i_{rd+}^+ \\ i_{rq+}^+ \\ i_{rd-}^- \\ i_{rq-}^- \end{bmatrix}
\tag{12}
$$

3. ROTOR FLUX SLIDING MODE OBSERVER AND MPPT CONTROL STRATEGY FOR DFIG

The aim of the control is to optimize the extraction of aerodynamic power (MPPT) under an unbalanced network voltage. The reference active power is determined as a function of the wind speed. So, based on the current model of the DFIG, a sliding mode full state observer is presented to estimate the rotor flux [22]-[23].

3.1. Rotor flux sliding mode observer

In this section, we present the rotor flux sliding mode observer for the MPPT control with rotor flux regulation. The simplicity and ease of implementation among the advantages of this observer. Figure 3 shows the structure of the rotor flux observer.
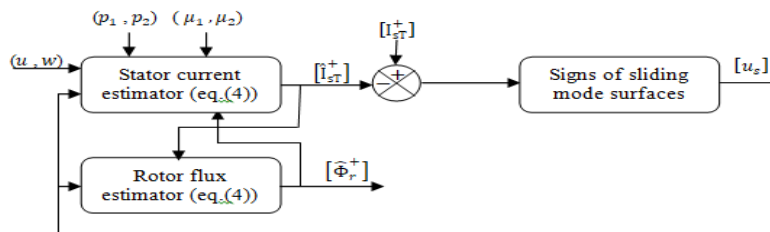

Figure 3. Rotor flux sliding mode observer structure

Let us rewrite the DFIG model (4) in the following form:

$$\begin{cases} \dot{I}_{sT}^+ = A_1 I_{sT}^+ + B_1 \Phi_r^+ + \delta u - \beta w \\ \dot{\Phi}_r^+ = \alpha M I_{sT}^+ + B_2 \Phi_r^+ + w \end{cases} \tag{13}$$

With $A_1 = \begin{bmatrix} -\eta & \omega_s \\ -\omega_s & -\eta \end{bmatrix}$; $B_1 = \beta \begin{bmatrix} \alpha & \omega \\ -\omega & \alpha \end{bmatrix}$; $B_2 = \begin{bmatrix} -\alpha & g\omega_s \\ -g\omega_s & -\alpha \end{bmatrix}$; $\delta = \frac{1}{\sigma L_s}$; $I_{sT}^+ = [\ i_{sTd}^+\ i_{sTq}^+\ ]^T$ and $\Phi_r^+ = [\ \varphi_{rd}^+\ \varphi_{rq}^+\ ]^T$

Hence, the structure of the observer can be expressed by [22]-[23]:

$$\begin{cases} \dot{\hat{I}}_{sT}^+ = A_1 \hat{I}_{sT}^+ + B_1 \widehat{\Phi}_r^+ + \delta u - \beta w + D_i u_s \\ \dot{\widehat{\Phi}}_r^+ = \alpha M \hat{I}_{sT}^+ + B_2 \widehat{\Phi}_r^+ + w + D_\Phi u_s \end{cases} \tag{14}$$

The dynamics of the estimation error are expressed by the following equations:

$$\begin{cases} \dot{\tilde{I}}_{sT}^+ = A_1 \tilde{I}_{sT}^+ + B_1 \widetilde{\Phi}_r^+ - D_i u_s \\ \dot{\widetilde{\Phi}}_r^+ = \alpha M \tilde{I}_{sT}^+ + B_2 \widetilde{\Phi}_r^+ - D_\Phi u_s \end{cases} \tag{15}$$

With : $\tilde{I}_{sT}^+ = I_{sT}^+ - \hat{I}_{sT}^+$; $\widetilde{\Phi}_r^+ = \Phi_r^+ - \widehat{\Phi}_r^+$; $u_s = [sign(S_1)\ \ sign(S_2)]^T$; $S = [S_1\ \ S_2]^T = \tilde{I}_{sT}^+$
S is the sliding mode surface and $(D_i\ ;\ D_\Phi)$ are the matrixes (2x2) that we will determine later.
Consider the Lyapunov candidate function $V_s = \frac{1}{2} S^T S$, we obtain:

$$\dot{V}_s = S^T \dot{S} = S^T \dot{\tilde{I}}_{sT}^+ = S^T (A_1 \tilde{I}_{sT}^+ + B_1 \widetilde{\Phi}_r^+) - S^T D_i u_s \tag{16}$$

in order to satisfy the condition of attractiveness ($S^T \dot{S} < 0$) , we must have

$$S^T (A_1 \tilde{I}_{sT}^+ + B_1 \widetilde{\Phi}_r^+) < S^T D_i u_s \tag{17}$$

If we put: $D_i = \begin{bmatrix} \mu_1 & 0 \\ 0 & \mu_2 \end{bmatrix}$. Then we obtain the condition below

$$\mu_1 |S_1| + \mu_2 |S_2| > S^T (A_1 \tilde{I}_{sT}^+ + B_1 \widetilde{\Phi}_r^+) \tag{18}$$

When the sliding mode is reached, the switching surface will verify it: $\dot{\tilde{I}}_{sT}^+ = \tilde{I}_{sT}^+ = 0$

Therefore, we obtain: $u_s = D_i^{-1} B_1 \widetilde{\Phi}_r^+ \tag{19}$
Introducing (19) in (15), we obtain

$$\dot{\widetilde{\Phi}}_r^+ = (B_2 - D_\Phi D_i^{-1} B_1) \widetilde{\Phi}_r^+ \tag{20}$$

We put : $-B_2 + D_\Phi D_i^{-1} B_1 = P \tag{21}$

Equation (20) becomes: $\dot{\widetilde{\Phi}}_r^+ = -P \widetilde{\Phi}_r^+$

In order to have exponential convergence, we choose P in the following form: $P = \begin{bmatrix} p_1 & 0 \\ 0 & p_2 \end{bmatrix}$

Where p_1 and p_2 are positive constants.

Finally, (21) can be rewritten as follows: $D_\Phi = (\begin{bmatrix} p_1 & 0 \\ 0 & p_2 \end{bmatrix} + B_2) B_1^{-1} \begin{bmatrix} \mu_1 & 0 \\ 0 & \mu_2 \end{bmatrix}$

To complete the design of this observer, we must choose the convenable observer parameters. We note that the $(p_1; p_2)$ parameters determine the dynamics of observer convergence and the $(\mu_1; \mu_2)$ parameters verify the conditions of attractiveness and stability of the observer.

3.1. Maximum wind power extraction

In order to capture the maximum power of the incident wind, we must adjust the rotational speed of the turbine permanently to the winds. The optimum operation speed of the generator is estimated for $\lambda_{opt} = 8,2$ by:

$$\omega_{opt} = \frac{G\,V_w\,\lambda_{opt}}{R} \tag{22}$$

Where G is Gearbox ratio of the wind turbine.

3.2 Backstepping control design under unbalanced grid voltage conditions

The control objective is twofold: the objective of higher priority is tracking the references trajectory (P_{s-ref}, Q_{s-ref}) where P_{s-ref} is the optimal stator active power reference according to optimal speed of the generator and the second is to keep the rotor flux at its nominal value by controlling the stator reactive power given via (27) regardless of the asymmetric voltage.

Using stator voltage orientation approach, i.e. $V_{sTd+}^+ = 0$, the rotor current references can be considered for eliminating the double frequency pulsations of stator output active power ($P_{s-sin2} = P_{s-cos2} = 0$). According to (11-a), the references of the positive and negative sequence rotor currents are calculated as [19]:

$$i_{rd+\_ref}^+ = \frac{-L_s v_{sTq+}^+}{MD_1} Q_{s0} + \frac{v_{sTq+}^+}{M\omega_s} \tag{23}$$

$$i_{rq+\_ref}^+ = \frac{-L_s v_{sTq+}^+}{MD_2} P_{s0} \tag{24}$$

$$i_{rd-\_ref}^- = \frac{\left[v_{sTq}^- i_{rd+}^+ - v_{sTd}^- i_{rq+}^+\right]}{v_{sq+}^+} - \frac{2v_{sTq-}^-}{M\omega_s} \tag{25}$$

$$i_{rq-\_ref}^- = -\frac{\left[v_{sTd}^- i_{rd+}^+ + v_{sTq}^- i_{rq+}^+\right]}{v_{sTq+}^+} + \frac{2v_{sTd-}^-}{M\omega_s} \tag{26}$$

With: $D_1 = v_{sTq+}^{+2} + v_{sTd-}^{-2} + v_{sTq-}^{-2}$ and $D_2 = v_{sTq+}^{+2} - (v_{sTd-}^{-2} + v_{sTq-}^{-2})$

And $P_{s-ref} = P_{s0}$. Also, equations (6) and (23) indicate respectively that the rotor flux and the stator reactive power Q_{s0} can be controlled by the d+ axis rotor current components ($i_{rd+\_ref}^+$), using (6)-(23)-(24)-(25) and (26), the signal reference ($\emptyset_{ref}$) of the rotor flux magnitude $\left(\sqrt{\varphi_{rd}^{+2} + \varphi_{rq}^{+2}}\right)$ can be expressed according the reactive power reference Q_{s0} by:

$$\emptyset_{ref}^2 = \left[L_r\sigma\left(\frac{-L_s v_{sTq+}^+}{MD_1}Q_{s0} + \frac{v_{sTq+}^+}{M\omega_s} + i_{rd-}^+\right) + \frac{M\varphi_{sq}^+}{L_s}\right]^2 + \left[L_r\sigma i_{rq}^+\right]^2 \tag{27}$$

From (27), Q_{s0} can be easily extracted (for $\emptyset_{ref} = 0,45$ Wb).

Using (7), (23), (24), (25) and (26) the errors dynamic equations are given by:

$$\dot{e}_1 = \frac{-L_s v_{sq+}^+}{MD_1}\dot{Q}_{s0} - \frac{1}{\sigma L_r}\left[v_{rd+}^+ - R_r i_{rd+}^+ + \omega_{slip+}\varphi_{rq+}^+\right] \tag{28}$$

$$\dot{e}_2 = \frac{-L_s v_{sq+}^+}{MD_2}\dot{P}_{s0} - \frac{1}{\sigma L_r}\left[v_{rq+}^+ - R_r i_{rq+}^+ - \omega_{slip+}\varphi_{rd+}^+\right] \tag{29}$$

$$\dot{e}_3 = \frac{d}{dt}\left(\frac{v_{sTq}^- i_{rd+}^+ - v_{sTd}^- i_{rq+}^+}{v_{sTq+}^+} - \frac{2v_{sTq-}^-}{M\omega_s}\right) - \frac{1}{\sigma L_r}\left[v_{rd-}^- - R_r i_{rd-}^- + \omega_{slip-}\varphi_{rq-}^-\right] \tag{30}$$

$$\dot{e}_4 = -\frac{d}{dt}\left(\frac{v_{sTd-}^- i_{rd+}^+ + v_{sTq-}^- i_{rq+}^+}{v_{sTq+}^+} - \frac{2v_{sTd-}^-}{M\omega_s}\right) - \frac{1}{\sigma L_r}\left[v_{rq-}^- - R_r i_{rq-}^- - \omega_{slip-}\varphi_{rd-}^-\right] \tag{31}$$

Consider the Lyapunov candidate function

$$V = \frac{1}{2}e_1^2 + \frac{1}{2}e_2^2 + \frac{1}{2}e_3^2 + \frac{1}{2}e_4^2 \tag{32}$$

To attain the objectives of tracking performance, the control signals v_{rd+}^+, v_{rq+}^+, v_{rd-}^- and v_{rq-}^- can be extracted from (28), (29), (30) and (31) satisfying $\dot{V}<0$ [19]:

$$v_{rd+}^+ = \sigma L_r\left[k_1 e_1 - \frac{L_s v_{sTq+}^+}{MD_1}\dot{Q}_{s0}\right] + R_r i_{rd+}^+ - \omega_{slip+}\varphi_{rq+}^+ \tag{33}$$

$$v_{rq+}^+ = \sigma L_r\left[k_2 e_2 - \frac{L_s v_{sTq+}^+}{MD_2}\dot{P}_{s0}\right] + R_r i_{rq+}^+ + \omega_{slip+}\varphi_{rd+}^+ \tag{34}$$

$$v_{rq+}^+ = \sigma L_r\left[k_2 e_2 - \frac{L_s v_{sTq+}^+}{MD_2}\dot{P}_{s0}\right] + R_r i_{rq+}^+ + \omega_{slip+}\varphi_{rd+}^+ \tag{35}$$

$$v_{rq-}^- = \sigma L_r\left[k_4 e_4 - \frac{d}{dt}\left(\frac{v_{sTd-}^- i_{rd+}^+ + v_{sTq-}^- i_{rq+}^+}{v_{sTq+}^+} - \frac{2v_{sTd-}^-}{M\omega_s}\right)\right] + + R_r i_{rq-}^- + \omega_{slip-}\varphi_{rd-}^- \tag{36}$$

Where k_1, k_2, k_3 and k_4 are positive constants. Introducing (33), (34), (35) and (36) in (32), the time derivative of the candidate Lyapunov function becomes negative definite: $\dot{V} = -k_1 e_1^2 - k_2 e_2^2 - k_3 e_3^2 - k_4 e_4^2 < 0$. This assures the global asymptotic stability of the error system. Based on the proposed control law described by (33), (34), (35) and (36), Figure 4 shows the schematic diagram of the control system for a DFIG.
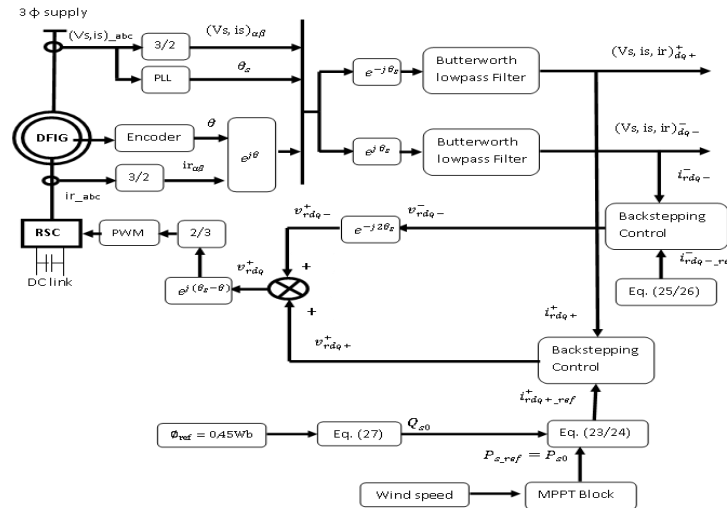

Figure 4. The schematic diagram of the proposed control

4. SIMULATIONS RESULTS

In order to demonstrate the performance of the rotor flux sliding mode observer, the simulation procedure is designed to consider a constant rotor flux (equal to its nominal value : $\emptyset_{ref} = 0,45$ Wb). The observer parameters (p_1, p_2) and (μ_1, μ_2) are chosen as follows: $p_1 = 200$, $p_2 = 60$, $\mu_1 = 1000$ and $\mu_2 = 1000$. Figure 5 shows the satisfactory performances of the rotor flux estimation. The estimated rotor flux tracks the actual rotor flux with good precision and the estimation error obtained is practically zero.

| Table I : Turbine parameters		Table II : DFIG parameters of DFIG 4 kW	
Number of blades	3	Number of poles pairs of the DFIG	2
Turbine radius, R (m)	3	Stator resistance	1.25 Ω
Gear box ratio	1:8.5	Stator leakage inductance	0.00096 H
Power	5 kW	Rotor resistance	0.17Ω
Cut-in wind speed	4.25 m/s	Rotor leakage inductance	0.0018 H
Rated wind speed	10.5 m/s	Mutuelle inductance	0.0772 H
Rotor inertia	0.05 kg m2	Viscous friction coefficient	0.001 m/s
		Generator inertia	0.33 kg m2
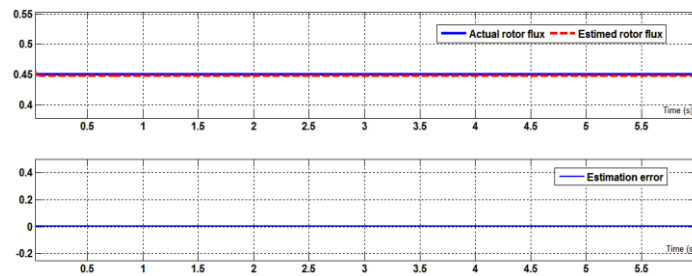
Figure 5. Rotor flux estimation results. Upper: Actual and estimated rotor flux; lower: estimation error

4.2. Controllers performances

The stimulation procedure is designed in such a way: during (0s-2s), the conventional Backstepping control was established during steady state (under the stable grid). Then at 2s, we started an asymmetric fault (a 20% of the nominal grid voltage dip of V_{sa}) to show the impact of the asymmetric fault on various signals of DFIG (with the conventional control). At the end, for (4s-7s) we show the feasibility of the enhanced Backstepping control based on the control law described by (33), (34), (35) and (36). The control parameters are chosen as follows: $k_1 = 30$, $k_2 = 120$, $k_3 = 115$ and $k_4 = 500$. The satisfactory performances of the stator active and reactive power tracking are shown in Figure 6.b and Figure 6.d by limiting the mechanical stress induced by asymmetrical fault. Also, note that for imposing a constant rotor flux, the stator reactive power reference is imposed according to (27), see Figure 6.c.We see that the error values remains practically zero
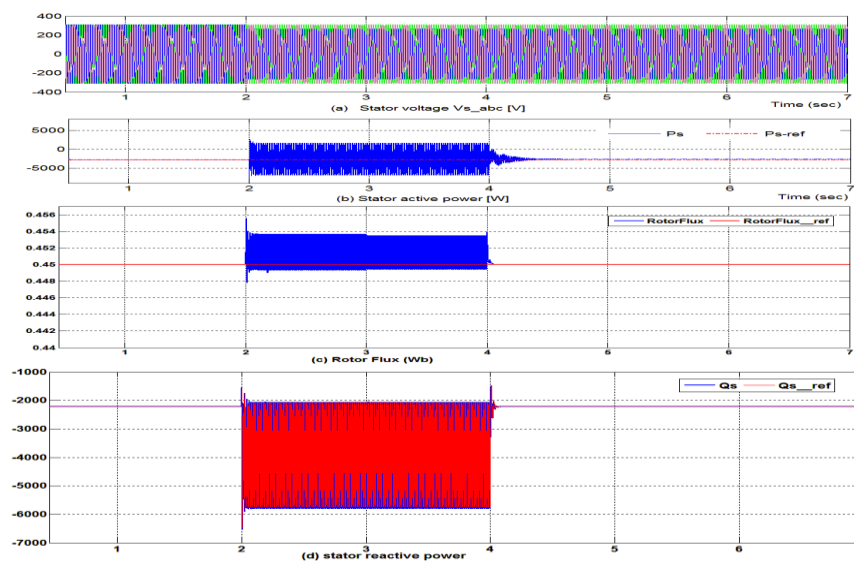

Figure 6. Simulation responses for 20% of depth of V_{sa}

5.   CONCLUSION

In this article, an improved MPPT control is developed using backstepping technique under unbalanced grid voltage associated with a rotor flux observer based on the sliding mode approach. The fault mode is activated when an asymmetric fault occurs in the grid voltage in order to eliminate the oscillations of the signals. Reference rotor currents are calculated, in order to maintain safe operation, as today's grid codes require. The proposed rotor flux observer is based on measuring electrical signals (stator currents, rotor and stator voltages). The performance and stability of control laws and observer have been shown by simulation studies in Matlab/Simulink® environment.

REFERENCES

[1]   Y. Majdoub, *et al.*, "Variable Speed Control of DFIG-Wind Turbine with Wind Estimation," *IEEE IRSEC conf., International Renewable and Sustainable Energy conference*, October 2014,pp. 268–274.
[2]   B. Purwahyudi, et al., "RNN Based Rotor Flux and Speed Estimation of Induction Motor," *International Journal of Power Electronics and Drive System (IJPEDS)*, Vol.1, N° 1, 2011, pp. 58-64.
[3]   A. Benheniche, et al., "A High Gain Observer Based Sensorless Nonlinear Control of Induction Machine," *International Journal of Power Electronics and Drive System (IJPEDS)*, Vol. 5, N° 3, 2015, pp. 305-314.
[4]   H. Echeikh, et al., "Online Adaptation of Rotor Resistance based on Sliding Mode Observer with Backstepping Control of A Five-Phase Induction Motor Drives," *International Journal of Power Electronics and Drive System (IJPEDS)*, Vol. 7, N° 3, 2016, pp. 648-655.
[5]   Renukrishna B., et al., "Sensorless Vector Control of Induction Motor Drives using Rotor Flux Observer," *IEEE International Conference on Power Electronics, Drives and Energy Systems*, December 2012.
[6]   G.Lefebvre, et al., "Electrical parameter observation for induction machine sensorless drive using a sensitivity and observability based EKF," *IEEE International Power Electronics and Motion Control Conference (PEMC)*, 2016, pp. 806 - 811.
[7]   G. Rigatos, "A derivative-free Kalman Filtering approach for sensorless control of nonlinear systems," *IEEE International Symposium on Industrial Electronics*,   2010, pp. 2049 - 2054.
[8]   Y. Zhou, *et al.*, "Operation of Grid-Connected DFIG Under Unbalanced Grid Voltage Condition," *IEEE Transactions ON Energy Conversion*, Vol. 24, No. 1, March 2009.
[9]   M. Farshadnia, *et al.*, "Current-based direct power control of a DFIG under unbalanced grid voltage," *Electrical Power and Energy Systems*, vol.62, 2014, pp. 571–582.
[10]   J. Hu, *et al.*, " DFIG wind generation systems operating with limited converter rating considered under unbalanced network conditions-Analysis and control design", *Renewable Energy*, vol. 36, 2011, pp. 829-847.
[11]   N. Amuthan, *et al.*, " Voltage sag ride through using Improved Adaptive Internal Model Controller for doubly fed induction generator wind farms", *Computers and Electrical Engineering*, 2013.
[12]   J. Hu, *et al.*, "Enhanced control of DFIG used back-to-back PWM VSC under unbalanced grid voltage conditions," *J Zhejiang Univ Sci A,*vol. 8(8), 2007, pp.1330-1339.
[13]   B. I. Nass, et al., " Methods for Reduction of Voltage Unbalance in Weak Grids Connected to Wind Plants". *IEEE Workshop on Wind Power and the Impacts on Power Systems*, 2002.
[14]   L. Xu, "Coordinated Control of DFIG's Rotor and Grid Side Converters During Network Unbalance," *IEEE Transactions on Power Electronics,*vol. 23, May 2008, pp.1041-1049.
[15]   L. Fan, *et al.*, "Negative Sequence Compensation Techniques of DFIG-based Wind Energy Systems under Unbalanced Grid Conditions," *Power Electronics and Machines in Wind Applications (PEMWA)*, June 2009.
[16]   J. Hu, *et al.*, "Improved Control of DFIG Systems During Network Unbalance Using PI–R Current Regulators," *IEEE Transactions on Industrial Electronics*, vol. 56, no. 2, February 2009, pp.439-451.
[17]   P. Pura, *et al.*, "Direct Power Control of DFIG Connected to Unbalanced Power Grid," *Eighth International Conference and Exhibition on Ecological Vehicles and Renewable Energies*, 2013.
[18]   M. J. Zandzadeh, *et al.*, "Modeling and improvement of direct power control of DFIG under unbalanced grid voltage condition," *Electrical Power and Energy Systems*, vol. 59, 2014, pp. 58–65.
[19]   Y. Majdoub, A. Abbou , M. Akherraz, R. El akhrif "Intelligent Backstepping Control of Variable Speed DFIG-Wind Turbine under unbalanced grid voltage conditions using Genetic Algorithm optimization," *International Review of Electrical Engineering (IREE)*, vol. 10, No 6, 2015, pp.716-726.
[20]   I. Boldea, *et al.*, "The induction machine handbook," *CRC Press*; 2002.
[21]   J.O.M. Rubioa, *et al.*, "Maximizing the performance of variable speed wind turbine with nonlinear output feedback control," *Procedia Engineering*, vol. 35, 2012, pp.31-40.
[22]   MOUTCHOU et al., "MRAS-based sensorless speed backstepping control for induction machine, using a flux sliding mode observer," *Turkish Journal of Electrical Engineering & Computer Sciences*,vol 23, 2015,pp 187-200.
[23]   A. Bourek, et al., "Indirect Adaptive Fuzzy Sliding Mode Observer for Sensorless Induction Machine Drive," Electromotion, vol. 14, 2007, pp. 143-153.